Check for updates

Preparation and characterization of soybean oil-based waterborne polyurethane/acrylate hybrid emulsions for self-matting coatings†

Yeyun Meng,[ab] Peng Lv,[ab] Qi Liu,[ab] Bing Liao,[c] Hao Pang (ID) *[a] and Weiqu Liu*[a]

This work aims to explore the feasibility of self-matting coatings based on soybean oil. A novel reactive waterborne polyurethane (RWPU) dispersion containing unsaturated C=C double bonds was synthesized from epoxidized soybean oil (ESO). Subsequently, the RWPU dispersion was copolymerized with hard/soft monomers at different weight ratios to prepare polyurethane/acrylate (MPU) hybrid emulsions. The results reveal the gloss levels of MPUs to be as low as 3.3 gloss units at 60°. A scanning electron microscope and three-dimensional surface profilometer were employed to observe the morphology of the MPU-based films, and the relation between the surface roughness and gloss was determined. Further, thermal gravimetric analysis was conducted to determine the thermal stability of the MPU-based films, and the results denoted that these MPU-based films exhibited excellent thermal stability. Tensile tests indicated that the RWPU dispersion, which was copolymerized at a hard monomer weight of 30%, exhibited a good tensile strength of 13.2 MPa and a high elongation percentage of 578%. Furthermore, after one year, the MPU emulsions exhibited a narrow particle size distribution and their zeta potential values were approximately −30.0 mV, revealing the excellent storage stabilities (>one year) of all the MPU emulsions.

Introduction

Matting agents, also known as low-gloss agents or gloss control additives, are extensively used in surface coatings to produce finishes exhibiting decreased gloss and light reflection.[1] They are selected because they can effectively reduce the surface glare when used in schools, hospitals, and minimize visual distractions to allow staff or students to maintain their focus while performing challenging tasks in such environments. Therefore, various power matting materials have been developed, including the commonly used diatomites,[2] silica,[3] wax-treated silica,[4] and clay.[5] Regardless, the aforementioned power matting materials exhibit certain disadvantages. The preparation of matted surfaces using powdered abrasives or sandpaper is time-consuming and inconvenient. Also, uneven surfaces tend to lack aesthetic appeal. Consequently, effective, inexpensive, and environment-friendly matting materials have to be developed.

Water-based matting materials are currently preferred by the matting material manufacturers. Waterborne polyurethanes

(WPUs) enjoy a preeminent status among the available coatings because they emit less volatile organic compounds (VOCs). Therefore, considerable research efforts have been devoted to develop low-gloss WPU coatings. Gao *et al.* used isophorone diisocyanate (IPDI) and adipate glycol (PBAG) to synthesize WPU dispersions containing different amounts of trimethylol-propane (TMP) and/or 2-[(2-aminoethyl)amino]ethane sulfonic acid sodium salt (AAS salt).[6] In cooperation with Yong *et al.*, a series of low-gloss WPU acrylate hybrid emulsions containing IPDI, polytetramethylene ether glycol (PTMEG), and acrylic monomers has been recently prepared.[7–10] A new low-gloss hybrid waterborne polyurethane dispersion comprising a self-matting material and a traditional silica-based matting material has been investigated by Uribe-Padilla *et al.*[11] However, the conventional method of producing low-gloss WPUs is usually based on the reaction between petroleum-derived polyols and isocyanates, which exhibits a large environmental footprint. The depletion of fossil fuels and stress of environmental pollution have led to an increasing focus on developing materials from renewable resources, which can provide various advantages, including reduced environmental impact, low cost, and potential biodegradability. To our best knowledge, few publications concerned the use of renewable resource to prepare self-matting coatings.

Hence, this work aims to synthesize vegetable-oil-based low-gloss WPU dispersions in accordance with the current trend of

[a] Guangzhou Institute of Chemistry, Chinese Academy of Sciences, Guangzhou 510650, China. E-mail: panghao@gic.ac.cn, liuwq@gic.ac.cn

[b] School of Chemistry and Chemical Engineering, University of Chinese Academy of Sciences, Beijing 100049, China

[c] Guangdong Academy of Sciences, Guangzhou 510650, China

† Electronic supplementary information (ESI) available. See DOI: 10.1039/c9nj04538d

searching for alternatives to petroleum-based materials.[12] By taking advantage of the vegetable-oil-based waterborne polyurethane as the matting material, strict VOCs emission requirements can be satisfied. Its good availability, low environmental impact, and cheap price make it promising for use in future applications. The objective of this research is to provide a novel method for the preparation of self-matting WPUs. In brief, epoxidized soybean oil (ESO) was used as the raw material to prepare soybean oil-based reactive waterborne polyurethane (RWPU). Subsequently, the RWPU dispersion copolymerized with hard/soft monomers at different weight ratios was used to yield polyurethane/acrylate hybrid emulsions (MPUs). The resultant MPU-based films were observed to exhibit low gloss, excellent thermal stability, and good tensile strength. The low-gloss effect of the MPU-based films was self-generated by the emulsion without the addition of any matting additives. It should be note that the self-matting coating are not based on 100% renewable resource.

Experimental

Materials

Epoxidized soybean oil (ESO) and other reagents including styrene (ST, 99%), methyl methacrylate (MMA, 98%), 2-ethylhexyl acrylate (2-EHA, 99%), butyl acrylate (BA, 99%), sodium dodecyl sulfonate (SDS, 99%), the emulsifier OP-10, potassium persulfate (KPS, 99.99%), isophorone diisocyanate (IPDI, 99%), dibutyltin dilaurate (DBTDL), dimethylolpropionic acid (DMPA, 98%), tetrafluoroboric acid (HBF4, >40%), 2-hydroxyethyl acrylate (HEA, 96%), and triethylamine (TEA, 99%) were all purchased from Aladdin China and used as received. Waterborne polyurethane/acrylic hybrid emulsion (BY-992) was purchased from Dongguan Yibao Resin Co., Ltd.

Synthesis of the soybean oil-based polyol

Methoxylated soybean oil-based polyol (MESO) was synthesized *via* the ring opening of ESO using methanol.[13,14] ESO (100 g) was added to a flask equipped with a mechanical stirrer and a dropping funnel. Methanol (100 g) and fluoroboric acid (1 g) were then added dropwise to the flask, and the mixture was vigorously stirred for 3 h at 50 °C; subsequently, methanol was eliminated *via* rotary evaporation under reduced pressure, and the main product was dried at 40 °C for 24 h in a vacuum oven. MESO was obtained as a clear and viscous liquid (98.4 g, yield: 86.3%). The number of hydroxyl groups in MESO was determined *via* acetic anhydride acetylation.[15]

Synthesis of the RWPU emulsion

MESO (25 g), IPDI (15.47 g), and DMPA (4.26 g) as well as the DBTDL catalyst (0.1 wt% based on total solids) were added to a 250 mL round-bottom flask equipped with a mechanical stirrer, a thermometer, a condenser with a drying tube, and an inlet for highly pure N2. The mixture was stirred at 75 °C for 4 h and cooled to 65 °C, and HEA (8.08 g) was added into the reactor for a further reaction time of 2 h. Subsequently, the mixture was
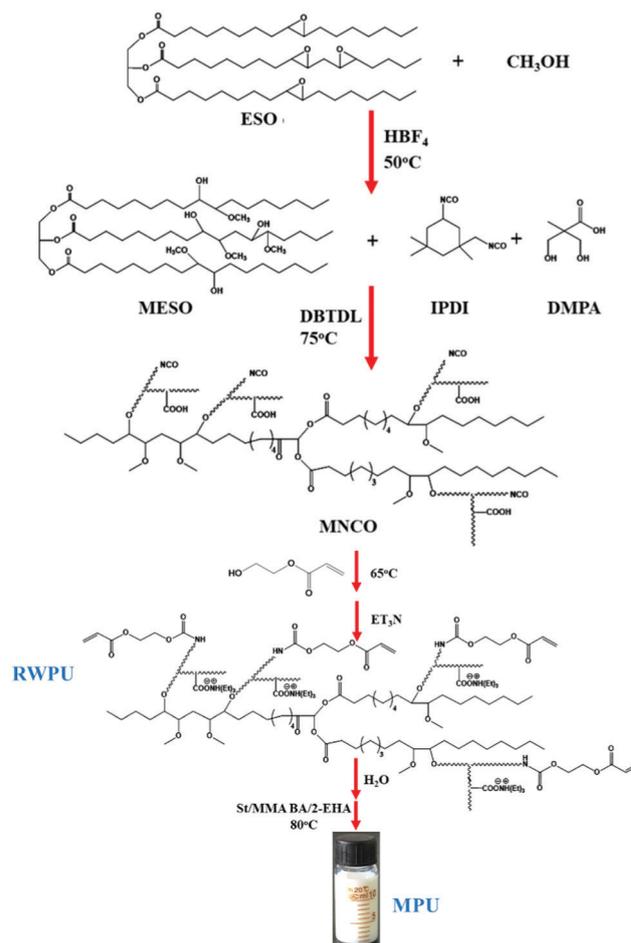

Fig. 1 Synthetic route to develop soybean oil-based polyol and the polyurethane/acrylate hybrid emulsion (MPU).

cooled to room temperature, and 3.86 g of TEA (1.2 equiv. per DMPA) was added; the mixture was stirred for another 30 min to neutralize the carboxylic groups of the DMPA. Finally, 100 mL of deionized water was added, and the mixture was stirred for the final 30 min at a stirring rate of 600 rpm. The methodology used to prepare the RWPU dispersion is shown in Fig. 1.

Synthesis of polyurethane/acrylate hybrid emulsions (MPU)

According to our previous work, hard monomers (MMA, and St) and soft monomers (BA, and 2-HEA) are contributed to low-gloss.[7–10] Polyacrylates have lower refractive index,[16] MMA and St act to enhance hardness, BA and 2-HEA play an important role in toughening. In general, St, BA, 2-EHA, MMA, and a stoichiometric amount of the synthesized RWPU dispersion were pre-emulsified using deionized water and emulsifier (1% on the basis of the total monomer weight) at room temperature for 30 min. Subsequently, 30% of the pre-emulsion was collected, and the flask was initially heated to 70 °C. A solution of the initiator was prepared by dissolving KPS (0.5% on the basis of the total monomer weight) in 20 mL of deionized water. Approximately one-third of the aqueous solution of KPS was added dropwise into the flask over a period of 30 min, and the

reaction temperature was increased to 80 °C. At this temperature, the extracted pre-emulsion was added dropwise, and the remaining KPS aqueous solution was pumped into the flask for 3 h; finally, the reaction was maintained at this temperature for another 2 h. The MPU emulsion was obtained with a solid content of approximately 33.5%. The MPU emulsion was obtained with a solid content of approximately 33.5%. The detailed data on the mixing weight ratio of the copolymerized systems are presented in Table 1.

$$\text{Solid content} = m_1/m_0 \times 100\%,$$

m_0 is the weight of the initial (wet) sample and m_1 the weight following drying.

Table 1 Sample designation of the MPU emulsions

Sample	RWPU (wt%)	Hard monomers (wt%) St + MMA	Soft monomers (wt%) BA + 2-EHA
RWPU	50	0	0
MPU1	50	25	25
MPU2	50	27.5	22.5
MPU3	50	30	20
MPU4	50	32.5	17.5
MPU5	50	35	15

Preparation of the MPU-based films

MPU-based films with a total thickness of approximately 1.0 mm were prepared by pouring the aqueous emulsions into Teflon molds. Then, drying at room temperature for 12 h, subsequently, the films were dried in a vacuum oven at 50 °C for another 12 h. The films were taken from the mold after drying, which were stored in a desiccator at room temperature.

Characterization

FT-IR and ^{1}H NMR spectroscopy. Fourier transform infrared (FT-IR) spectra were recorded on a Nicolet 5100 spectrometer using KBr pellets as sample matrices in the fundamental spectral region of 500–4000 cm^{-1}. Meanwhile, ^{1}H NMR spectra were recorded on a DRX-300 MHz (Bruker) superconducting-magnet nuclear magnetic resonance (NMR) spectrometer. The chemical shifts were recorded relative to that of deuterated chloroform (δ = 7.26 ppm).

Gloss measurements. Gloss measurements were performed using a portable gloss meter (KGZ-60, Tianjin Yaxing). All of these measurements were made at 60° for each film. The values of gloss were measured five times for each sample and the average gloss was reported.

Surface analysis. The surface morphology of the MPU-based films was characterized with an S-4800N scanning electron microscope (SEM) system at 15 kV. The dried films were stained on a sample stage with a conductive adhesive. The samples for SEM were covered with a thin layer of gold prior to analysis. In addition, the surface roughness of MPU-based films was performed using a 3D Surface Profilometer (BMT EXPERT). The film was prepared by casting a certain amount of emulsion onto a mold with a 100 mm × 60 mm × 3 mm smooth Teflon groove.

The morphology of MPU-based films was also revealed by Atomic Force Microscopy (AFM, NanoManVS).

Particle size. The particle size distribution was observed by a laser diffraction size analyzer (Malvern Nano ZS90) in dynamic light scattering mode. Zeta potential measurement was carried out *via* electrophoresis (Malvern Nano-ZS90) at 25 °C. Prior to the measurements, the RWPU and MPU emulsions were diluted with deionized water to a concentration of 3000 ppm.

Thermal analysis. Thermogravimetric (TG) was carried out using a NETZSCH TG 209 F3 analyzer under a nitrogen flow. Samples were heated from room temperature to 800 °C at a rate of 10 °C min^{-1} under a nitrogen atmosphere. The weight loss and the first derivative weight were recorded as a function of the temperature.

Gas chromatography (GC). The residual monomers were analyzed by gas chromatography spectrometry (QP-2010, Shimadzu, Japan). The MPUs emulsions were separately extracted with toluene and transferred into a volumetric flask for analysis.

Tensile strength and elongation at break. The tensile properties of films were measured using a universal testing machine (RGM-3030) at 20 mm min^{-1} crosshead speed. Films were both made into dumbbell shape with 1.0 mm thickness. The adhesion strength of the films was tested by cross-cut adhesion method, according to ASTM D3359. The result was presented using a rating of 0B for a low adhering coating through 5B for a high adhering.

Results and discussion

Chemical structural characterization

MESO, RWPU, and MPU copolymer were synthesized as shown in Fig. 1. According to the FTIR spectra of ESO and MESO shown in Fig. 2, hydrogen bonding is a very important feature in MESO, where a single stretching band can be observed in its spectrum at approximately 3450 cm^{-1}, which corresponds to the hydrogen-bonded O–H stretching vibration. The peak at 830 cm^{-1} was monitored, and its disappearance was attributed to the consumption of epoxide moieties, which indicated the successful synthesis of MESO. After the hydroxyl groups of MESO
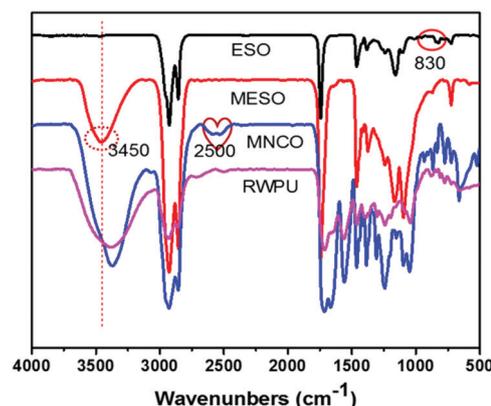

Fig. 2 FTIR spectra of pure soybean oil (ESO), methoxylated soybean oil-based polyol (MESO), MNCO (MESO reacted with isophorone diisocyanate), and RWPU.
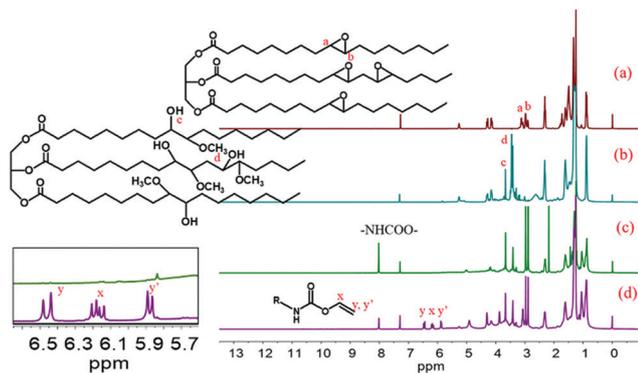
Fig. 3 ^{1}H NMR spectra of (a) pure soybean oil (ESO), (b) methoxylated soybean oil-based polyol (MESO), (c) MNCO (MESO reacted with isophorone diisocyanate), and (d) RWPU.

reacted with the diisocyanate groups of IPDI, the characteristic band could still be observed at approximately 2500 cm^{-1} (–NCO). The subsequent disappearance of this peak indicated the successful synthesis of RWPU *via* the reaction between the hydroxyl groups in HEA and residual –NCO in MNCO.

The MESO and RWPU chemical structures were confirmed by ^{1}H NMR, depicted in Fig. 3. As can be seen in the spectrum of ESO, shown in Fig. 3a, resonance can be observed in the peak of *a* and *b* (2.8–3.2 ppm), which can be ascribed to the epoxide groups. In the spectrum shown in Fig. 3b, resonance can be observed in the peak of *c* and *d* (3.4–3.7 ppm), which can be attributed to the hydrogen-bonded O–H and methoxy groups of MESO because of the reaction between ESO and methanol. The characteristic resonance of diisocyanate (–NHCOO–) groups at 8.0 ppm can also be observed in the spectrum, as shown in Fig. 3c. These results indicate that the isocyanate groups successfully react with different hydroxyl groups. In addition, in the RWPU spectrum, shown in Fig. 3d, a strong peak that can be observed in the 5.7–6.5 ppm region corresponds to the unsaturated –C=C–H group of HEA.

Thermal analysis

The thermal stabilities of the RWPU and MPU films were determined by TGA under a nitrogen atmosphere. It is well known that the thermal degradation of polyurethanes occurs *via* a two- or three-stage process.[17,18] During the first stage, the degradation can be attributed to the decomposition of hard segments, leading to the formation of the isocyanate and alcohol groups, primary or secondary amines, olefins, and carbon dioxide.

The second and third stages correspond to the decomposition of soft segments.[19,20] The TGA and DTG curves are displayed in Fig. 4, and the detailed thermal decomposition data are summarized in Table 2. In case of the neat RWPU film, the three degradation stages are shown in Fig. 4b, where the first degradation step begins at 148 °C and the maximum degradation rate can be observed at 385 °C. In case of the MPU-based films, the second stage of degradation mainly occurs in 350–450 °C. These results reveal that the MPU-based films offer better thermal stability when compared with that offered by the RWPU film.
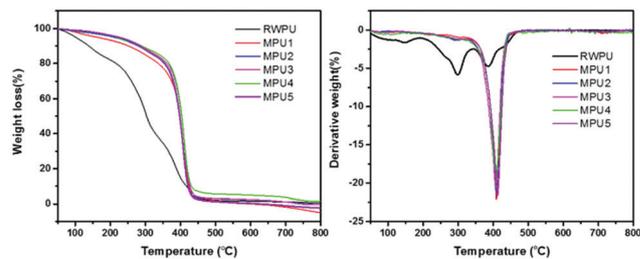

Fig. 4 TGA and DTG curves of the RWPU and MPU films.

Table 2 Thermal stabilities of the RWPU and MPU films

Sample	T5% (°C)	T50% (°C)	Tmax2 (°C)
RWPU	101	303	382
MPU1	163	398	409
MPU2	209	400	410
MPU3	227	403	408
MPU4	214	399	411
MPU5	221	401	414

Surface roughness

Gloss is an optical property which indicates how well a surface reflects light in a specular (mirror-like) direction. It is one of important parameters that are used to describe the visual appearance of an object. The factors that affect gloss are the refractive index of the material, the angle of incident light and the surface roughness.[21,22] The surfaces of the MPU-based films were observed by SEM, and the corresponding images are shown in Fig. 5. Heterogeneous phenomena can be observed on the surfaces of the MPU films, indicating that the copolymerized systems formed rough surfaces.

On the one hand, the refractive index of the material contributing to the low gloss. Polyacrylates have lower refractive index,[16] nevertheless, hard monomers have higher glass transition temperature, which act to enhance hardness. If only copolymerized with hard monomers, the films presented brittle and fragile. BA and 2-HEA play an important role in toughening.

On the other hand, gloss depends on the amount of specular reflection. When a beam of incident light is irradiated on a rough surface, majority of the light is either absorbed, diffused, or reflected in multiple ways on the film surface.[23,24]
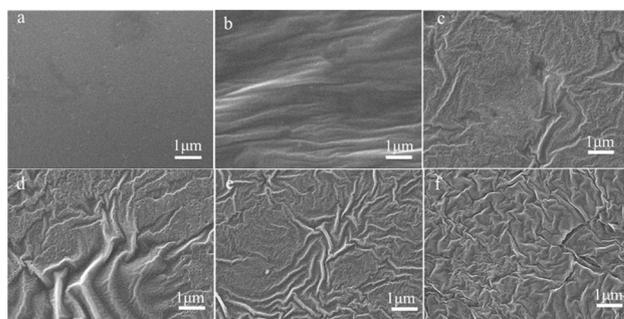

Fig. 5 SEM images of the MPU-based films: (a) RWPU; (b) MPU1; (c) MPU2; (d) MPU3; (e) MPU4; and (f) MPU5.
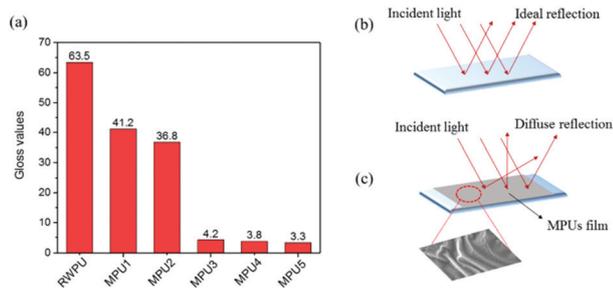
Fig. 6 Gloss values and matting mechanism. (a) The gloss values of the MPU-based films, (b) mirror-like surface with high gloss, and (c) rough surface with matting effect.

Table 3 The contents of unreacted volatile monomers in the MPU emulsions

Samples	MMA (%)	St (%)	BA (%)	2-HEA (%)
MPU1	0	38.8×10^{-4}	0	5.92×10^{-4}
MPU2	0	43.6×10^{-4}	0	0
MPU3	0	36.8×10^{-4}	0	8.82×10^{-4}
MPU4	0	52.7×10^{-4}	4.5×10^{-4}	0
MPU5	0	53.9×10^{-4}	5.76×10^{-4}	0

Therefore, only a small amount of light can be reflected to people's eyes, leading to a low-gloss effect.[25,26] In case of wavy surface roughness, the distribution of the reflected light is dependent on the degree of roughness.[27]

The results of low gloss value showed in Fig. 6. To explain how to create a rough film surface, a detailed discussion is presented in this research. Rough surfaces could be caused by the incompatibility of polyacrylate and waterborne polyurethane constituents, which leads to phase separation.[28] The microphase separated nanoscale morphology of the phase-separated MPUs was visualized by the AFM height and phase imaging of the smooth surfaces, the results of which are shown in Fig. 7. Soft segments are expected to be denoted as dark contrast in phase imaging, whereas hard segments are expected to be observed as bright areas.[29,30] Here, the hard segments exhibit a globule-like morphology and are distributed over the entire sample area. The hard microdomains self-aggregated from discrete to continuous morphology as the hard segment content increased. The gloss of MPU' films declined with the hard monomers increasing. This result could be due to the increment of contents of the hard segment, the degree of microphase separation increased, causing an unstable film-forming process and increasing the average surface roughness.[31–34] The possible reasons are as follows: (1) thermodynamically, phase separation is more complete with aromatic hard segments because of increased thermodynamic incompatibility between hard segments and aliphatic soft segments.[31] (2) From a kinetic viewpoint phase separation becomes more complete with hard segments because of increased. Phase separation was very fast as the hard-segment mobility was relatively high and the system viscosity was low.[35,36] (3) Low gloss also can be achieved by rough surfaces *via* the orange peel effect, which is caused by the quick evaporation of film. MPU emulsions is a heterogeneous system, which contains waterborne polyurethane copolymers, oligomers, and a small amount of residual monomers. The residual monomers evaporated with water, the oligomers dried rapidly, and the systems became increasingly viscous. The opposite is true in case of the waterborne polyurethane copolymers, which dry slowly, and is an important factor that contributes toward the results roughness occurs due to a mechanical mismatch between the surface of the film and its interior. The residual monomer content was determined by GC, the results of which are shown in Table 3. The results reveal that the unreacted volatile monomer content is very small. The residual MMA, BA, and 2-EHA contents are almost 0, which may be closely related to the reactivity ratios of the volatile monomers. Further, there is no evident pattern in the unreacted monomer contents of the MPU1, MPU2, MPU3, MPU4, and MPU5 samples.

To further explore the roughness of the MPU-based films, an investigation was conducted using a profilometer to evaluate the degree of roughness of the MPU films. In three-dimensional optical profilometry, roughness is usually expressed as the surface area roughness or S_a, which can be assessed from the root mean square roughness (R_q). It can be inferred from Fig. 8a–e that the roughness of the MPU-based films increases for films exhibiting high hard monomer content. This result is consistent with the SEM results. The R_q of MPU1, MPU2, MPU3, MPU4, and MPU5 were 0.25, 0.56, 0.97, 1.3, and 2.3 μm, respectively. Profile roughness (R_a) also can be extracted as a line through an area, which is evaluated based on the average wavelength (λ_a). Their λ_a were 7.0, 7.4, 7.8, 10.2, and 12.9 μm, respectively. The trends in R_a (shown in Fig. 8f–j) are similar to the trends in S_a.

Particle size distribution and zeta potential

Fig. 9a–f denote the particle size distributions of the RWPU and MPU emulsions, respectively. In contrast with the RWPU emulsion, the MPU hybrid emulsions exhibit considerably narrower particle distributions; moreover, the z-average particle sizes of all the emulsion samples were smaller than 100 nm, indicating that all the emulsion samples exhibited excellent stability. In addition, all the emulsion samples were observed to remain stable for more than a year. As shown in Fig. 10a–f, after one year, the particle size distribution of the RWPU and MPU emulsions, respectively. The z-average particle sizes of all the emulsion in Fig. 10a–f were
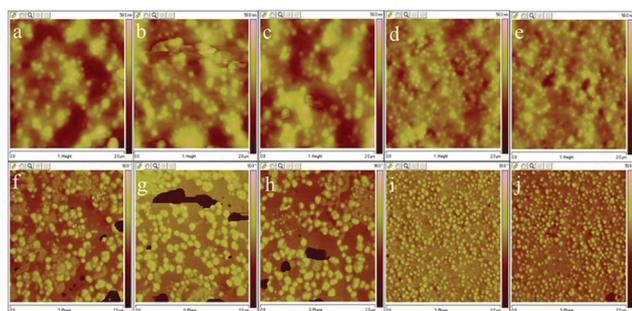

Fig. 7 (a–e) Height and (f–j) corresponding phase images obtained by AFM: (a and f) MPU1; (b and g) MPU2; and (c and h) MPU3; (d and i) MPU4; and (e and j) MPU5.
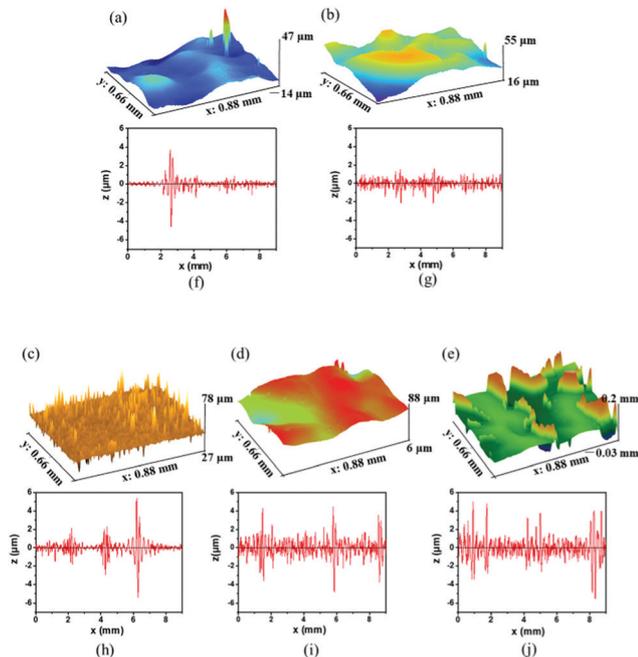
Fig. 8 3D profilometer images and line scanning curves of the MPU films. Surface area roughness of (a) MPU1, (b) MPU2, and (c) MPU3, (d) MPU4, and (e) MPU5 with R_q values of (a) 0.25, (b) 0.56, (c) 0.97, (d) 1.3, and (e) 2.3 μm, respectively. Line roughnesses of (f) MPU1, (g) MPU2, (h) MPU3, (i) MPU4, and (j) MPU5, where the λ_a values are (f) 7.0, (g) 7.4, (h) 7.8, (i) 10.2, and (j) 12.9 μm, respectively.
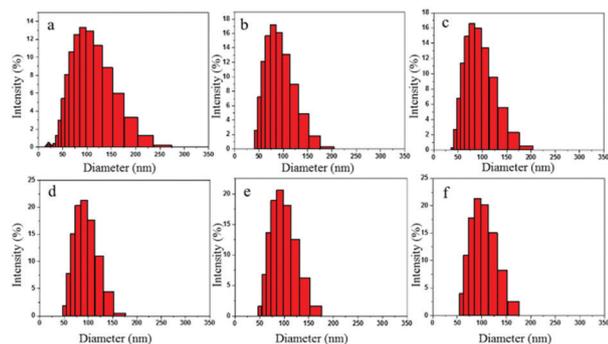
Fig. 9 Particle size distributions of the RWPU and MPU emulsions: (a) RWPU; (b) MPU1; (c) MPU2; (d) MPU3; (e) MPU4; and (f) MPU5.
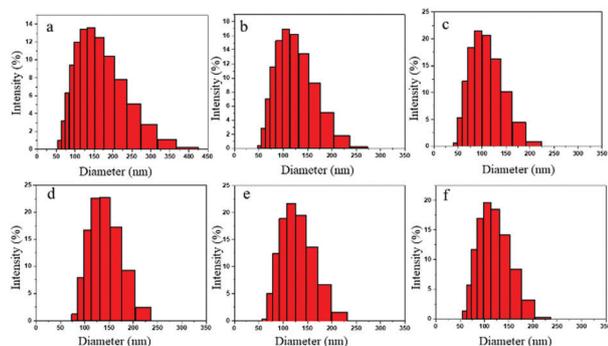
Fig. 10 Particle size distributions of emulsions after one year: (a) RWPU; (b) MPU1; (c) MPU2; (d) MPU3; (e) MPU4; and (f) MPU5.

Table 4 Zeta potential of the RWPU and MPU emulsions

| Sample	Zeta potential (mV)	Zeta potential after one year (mV)
RWPU	−46.2	−26.8
MPU1	−44.7	−30.8
MPU2	−42.6	−30.1
MPU3	−47.5	−30.7
MPU4	−46.5	−31.5
MPU5	−47.3	−32.6

larger than 100 nm. In particular, RWPU presented a broad distribution, indicating that the stability of the RWPU dispersion gradually decreased over time. Additional, zeta potential was used to examine the stability of RWPU and MPU emulsion, the results were summarized in the Table 4. The results indicated that the zeta potential values of all the emulsions decreased after one year. In spite of this, zeta potential values of MPU emulsions were approximately −30.0 mV, revealing the excellent storage stabilities (>one year) of all the MPU emulsions.

Tensile properties

From the tensile test results presented in Table 5, the specimen exhibit appreciably improved mechanical properties with the incorporation of hard monomers. In particular, the addition of hard monomers by up to 35% into the composites improves their tensile strength and Young's modulus but not the percentage of elongation. With an increase in the hard monomers content, the film becomes brittle and fragile, resulting in a decrease in the percentage of elongation of the sample. This result could attribute to the increase of the weight ratio of hard monomers, which contained many rigid phenyl skeleton structures. From the aforementioned results, RWPU is observed to copolymerize with an appropriate ratio of hard and soft monomers, exhibiting good tensile strength when compared with that exhibited by the neat RWPU.

Table 5 Mechanical and physical properties of the MPU films

Properties	Tensile strength (MPa)	Elongation at break (%)	Adhesion	Performance appearance of emulsion	Stabilities of emulsion
RWPU	26.3	124	4B	Light-blue	Over 12 months
MPU1	7.1	1304	5B	Milk-white	Over 12 months
MPU2	9.7	619	5B	Milk-white	Over 12 months
MPU3	13.2	578	5B	Milk-white	Over 12 months
MPU4	14.7	448	5B	Milk-white	Over 12 months
MPU5	28.4	122	5B	Milk-white	Over 12 months
BY-992	5.7	548	5B	Milk-white	Over 6 months
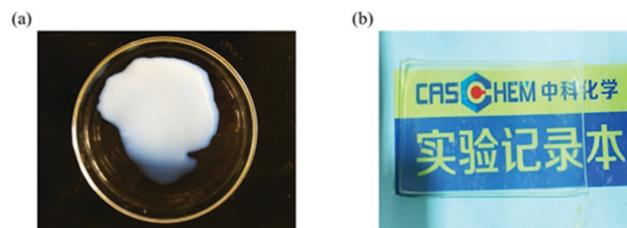
Fig. 11 The appearance of (a) the MPU3 dispersion and (b) the MPU3 film.

With respect to the peel adhesion, RWPU showed 4B degrees of adhesion strength, while the MPU films showed 5B degrees of adhesion strength. This result could attribute to rigid phenyl skeleton structures and the toughness of soft monomers. However, no significant change was observed when the hard monomer content was increased. Fig. 11 shows the appearance of the MPU3 dispersion and its film. A transparent film was formed after the milk-white MPU dispersion dried, which makes it promising for use in future applications the field of low-gloss materials.

Conclusions

In this study, low-gloss soybean oil-based waterborne polyurethane acrylate hybrid emulsions that produced films with variable rough surfaces were successfully synthesized. This study focused on the physical properties of the MPU films such as the gloss, thermal stability, and tensile strength. The surfaces of the MPU-based films spontaneously acquired roughness during the drying process. Based on the observations, it can be concluded that as the amount of hard monomer increases, the MPU-based films acquire a greater degree of roughness. Further, the results reveal that the thermal stability is improved and that gloss reduction is achieved owing to the introduction of soft and hard monomers. The gloss levels of the MPUs were observed to be as low as 3.3 gloss units at 60°. Furthermore, after one year, the MPU emulsions exhibited a narrow particle size distribution and their zeta potential values were approximately -30.0 mV, revealing the excellent storage stabilities ($>$ one year) of all the MPU emulsions. Therefore, RWPU copolymerized with an appropriate ratio of hard and soft monomers to exhibit low gloss, excellent thermal stability, and good tensile strength. Based on these observations, the soybean oil-based polyols can be considered to be promising candidates for the synthesis of a new class of renewable resource-based waterborne MPUs exhibiting low gloss for use in a wide range of industrial applications.

Conflicts of interest

There are no conflicts to declare.

Notes and references

1 S. E. Maskery, *Pigm. Resin Technol.*, 1973, **2**, 11.
2 Y. C. Du, S. L. Shi, C. Y. Bu, H. X. Dai, Z. G. Guo and G. Y. Tang, *Part. Sci. Technol.*, 2011, **29**, 368.
3 H. D. Christian, *Eur. Coat. J.*, 2006, **30**, 26Vincentz Network.
4 D. Aldcroft and G. J. Earl, *Eur. Pat.*, 1706, 1998.
5 J. Cawthorne, M. Joyce and D. Fleming, *J. Coat. Technol.*, 2003, **75**, 75.
6 X. Cao, X. Ge, H. Chen and W. Li, *Prog. Org. Coat.*, 2017, **107**, 5.
7 Q. Yong, H. Pang, B. Liao, W. Mo, F. Huang, H. Huang and Y. Zhao, *Prog. Org. Coat.*, 2018, **115**, 18.
8 Q. Yong, B. Liao, G. Ying, L. Caizhen, H. Huang and H. Pang, *J. Coat. Technol. Res.*, 2018, DOI: 10.1007/s11998-017-0030-7.
9 Q. Yong, B. Liao, J. Huang, Y. Guo, C. Liang and H. Pang, *Surf. Coat. Technol.*, 2018, DOI: 10.1016/j.surfcoat.2018.01.012.
10 Q. Yong, F. Nian, B. Liao, Y. Guo, L. Huang, L. Wang and H. Pang, *Polym. Bull.*, 2017, **74**, 1061.
11 J. Uribe-Padilla, M. Graells-Sobré and J. Salgado-Valle, *Prog. Org. Coat.*, 2017, **109**, 179.
12 S. K. Gaddam, S. N. Raju Kutcherlapati and A. Palanisamy, *ACS Sustainable Chem. Eng.*, 2017, **5**, 6447.
13 R. C. Larock and Y.-S. Lu, *Biomacromolecules*, 2008, **9**, 3332.
14 Z. S. Petrović, A. Guo and W. Zhang, *J. Polym. Sci., Part A: Polym. Chem.*, 2000, **38**, 4062.
15 ASTM D4274 – 99. 2014, 988.
16 M. Hébert, Reflection and transmission of light by a flat interface, Fresnel's formulae, 2013.
17 N. Ketata, C. Sanglar, H. Waton, S. Alamercery, F. Delolme, G. Raffin and M. F. Grenier-Loustalot, *Polym. Polym. Compos.*, 2005, **13**, 1.
18 V. Mamleev, S. Bourbigot, M. Le Bras, S. Duquesne and J. Šesták, *Phys. Chem. Chem. Phys.*, 2000, **2**, 4796.
19 J. Lu, F. Yan and J. Texter, *Prog. Polym. Sci.*, 2009, **34**, 431.
20 S. V. Levchik and E. D. Weil, *Polym. Int.*, 2004, **53**, 1585.
21 R. S. Ingersoll, *J. Opt. Soc. Am.*, 1921, **5**, 213.
22 R. S. Hunter, NBS Research Paper RP 958, *J. Res.*, 1937, **18**, 19.
23 N. J. Elton and J. C. C. Day, *Meas. Sci. Technol.*, 2009, **20**, 025303.
24 N. J. Elton, *J. Opt. A: Pure Appl. Opt.*, 2008, **10**, 085002.
25 J. Järnström, P. Ihalainen, K. Backfolk and J. Peltonen, *Surf. Sci.*, 2008, **254**, 5741.
26 S. K. Basu, L. E. E. Scriven, L. F. F. Francis and A. V. V. McCormick, *Prog. Org. Coat.*, 2005, **53**, 1.
27 G. Kigle-Boeckler, *Met. Finish.*, 1995, **93**, 28.
28 S. L. Giles, N. W. M. Heller, C. R. Clayton, M. E. Walker, M. J. Wytiaz and J. H. Wynne, *ACS Appl. Mater. Interfaces*, 2016, **8**, 26251.
29 P. Schön, K. Bagdi, K. Molnár, P. Markus, B. Pukánszky and G. J. Vancso, *Eur. Polym. J.*, 2011, **47**, 692.
30 E. Tocha, H. Janik, M. Debowski and G. J. Vancso, *J. Macromol. Sci., Part B: Phys.*, 2002, **41**, 1291.
31 Y. Li, W. Kang, J. O. Stoffer and B. Chu, *Macromolecules*, 1994, **27**, 612.
32 A. Nakajima, K. Abe, K. Hashimoto and T. Watanabe, *Thin Solid Films*, 2000, **376**, 140.
33 R. Zhu, X. Wang, J. Yang, Y. Wang, Z. Zhang, Y. Hou, F. Lin and Y. Li, *Appl. Sci.*, 2017, **7**, 306.
34 J. Li, W. Tsen, C. Tsou, M. Suen and C. Chiu, *Polymers*, 2019, **11**, 1333.
35 Y. Li, T. Gao and B. Chu, *Macromolecules*, 1992, **25**, 1737.
36 Y. Li, Z. Ren, M. Zhao, H. Yang and B. Chu, *Macromolecules*, 1993, **26**, 612.